HEIGHT ESTIMATION OF BUILDINGS FROM HIGH-RESOLUTION SAR DATA BASED ON INTERFEROMETRIC ANALYSIS

Kentaro Suzuki[1], Wen Liu[1], and Fumio Yamazaki[1]

[1]Chiba University, 1-33 Yayoi-cho, Inage-ku, Chiba 263-8522, Japan,
E-mail: kentaro_suzuki@chiba-u.jp; wen.liu@chiba-u.jp; fumio.yamazaki@faculty.chiba-u.jp

KEY WORDS: SAR, Interferometric analysis, TerraSAR-X, Building inventory, Building height

ABSTRACT: Building inventory is important information for monitoring urban development and evaluating risks from natural disasters. Building height is an essential element for inventory. Owing to the advancement of remote sensing technology, it is possible to detect building heights from high-resolution satellite images. In this study, the building heights in San Francisco, California, U.S.A. were estimated by an Interferometric SAR (InSAR) analysis and a geometric method from 1-m resolution TerraSAR-X's HighSpot data. Two Single Look Slant-Range Complex (SSC) data provided by the 2012 IEEE Date Fusion Contest were used. A flattened interferogram image was obtained after removing the phases caused by the elevation and baseline through the InSAR analysis. At first, the layover areas of buildings were extracted according to the phase information. Then, the building heights were calculated from the lengths of layover. The obtained result was verified by comparing with Lidar data, which was taken in June 2010. According to the comparison, the heights of high-rise buildings were found to be estimated successfully by the proposed method with high accuracy.

1. INTRODUCTION

Modeling and monitoring of urban areas are important for urban planning, environmental assessment and evaluating risks from natural disasters. Remote sensing technology has an advantage of observing a wide area periodically. In addition, synthetic aperture radar (SAR) does not depend on the weather condition, and can observe the earth surface at daytime and nighttime. Thus, periodical observation using SAR images is a useful method to monitor urban development. In the last few years, the high-resolution (HR) SAR sensors having approximately 1-m spatial resolution, e.g., COSMO-SkyMed and TerraSAR-X (TSX), are available and provide us more detailed earth surface information. It became possible to model the shape and estimate the height for an individual building in urban areas. Since the side-looking nature of SAR observation is suitable for detecting the height of vertical structures, several methods related to the height detection from SAR images have been proposed.

These methods can be divided into three types. The first category is based on a direct electromagnetic backscattering model. Franceschetti et al. (2002, 2007) proposed a method for extracting the building height information based on a radiometric analysis of the double-bounce contribution, and they tested this method upon an airborne SAR sensor image. Liu et al. (2009) applied the method to a TSX image of Shanghai, China. However, this method requires prior knowledge of the material and surface roughness properties of the background. Thus it was difficult to be used in different areas. The second category is based on geometrical characteristics due to oblique observation such as layover and radar shadow. The height estimation from a HR SAR image has the accuracy in a meter order. Brunner and Lemoine (2010) estimated building heights by matching simulated SAR images with a TSX image containing buildings of various heights. Liu and Yamazaki (2013) proposed a method to detect layover areas by a threshold value of the backscatter intensity and a 2D GIS data. Then the building heights were calculated from the length of the detected layover. The method was applied to a TSX image of San Francisco, U.S.A. and Lima, Peru (Yamazaki et al., 2013). However, the targets in these researches were only low-rise buildings. Due to the complicated reflection pattern of building walls and the influence from surrounding conditions, this method could not work well for the high-rise building which has a large layover area.

The third category is based on interferometric SAR (InSAR) analysis. Building heights could be estimated by removing elevation effects from a Digital Surface Model (DSM) built from a InSAR analysis result. Bolter and Leberl (2000) extracted buildings and their heights from multiple-view InSAR datasets. Thiel et al. (2007) used two approaches to detect buildings in different sizes from multi-aspect HR airborne InSAR datasets. Building features were extracted independently for each direction from the amplitude and phase information in InSAR data. However, the platform of these studies is airborne SAR, which is more expensive and thus less archive data. Although the InSAR analysis can measure the altitude in a centimeter order, it is difficult to estimate building heights due to the complicated environments in urban areas.

In this study, a method for detecting building heights is proposed using HR SAR images and a GIS building footprint data, on the basis of the InSAR analysis and geometrical characteristics. The study area is selected in San Francisco, California, U.S.A., and two TSX data are used. First, a flattened interference phase image is obtained by the InSAR analysis after removing orbital and topographic fringes. Secondly, the characteristics of phases in layover areas that are built according to the GIS data are investigated for several sample buildings. Then the parameters for layover extraction are summarized and applied to the other buildings. The building heights are estimated by the relationship of a vertical height and its layover length. Finally, the accuracy of the obtained results is verified by comparing with a Lidar data.

2. STUDY AREA AND IMAGERY DATA

The study area focuses on Skyscrapers zone of San Francisco, CA, U.S.A., as shown in Figure 1(a). Two TSX images were taken on December 5 and 27, 2007, respectively. The shooting area is shown in Figure 1(b) by a red square. The two images were taken in the descending path of 189.8° orbital angle (clockwise from the north) and by HH polarization with 0.031 m wavelength. Data were provided as Single Look Complex (SLC) product by the 2012 IEEE Date Fusion Contest. Since the images were captured in the HighSpot Mode (HS), the azimuth resolution was about 1.10 m and the slant-range resolution was about 0.92 m for a single look. A Digital Elevation Model (DEM) and a DSM taken by the aerial Lidar sensor were also provided by the 2012 IEEE Date Fusion Contest, which were used to remove elevation effects. The data area is shown in Figure 1(b) by a green frame. The vertical resolution of the Lidar data is 0.06 [m] and the spatial resolution 2.0 [m/pixel].

The SLC products were projected and calibrated by introducing the Lidar DEM, and were transformed into the geo-coded intensity images. The pre-processed image taken on December 5, 2007 is shown in Figure 2(a). Reference building heights were obtained by subtracting the DEM from the DSM, as shown in Figure 2(b). In addition, a GIS building footprint data were downloaded from the San Francisco government's homepage (2011) and shown in Figure 2(b) by white lines. There are 1,704 buildings in the study area, and twelve high-rise buildings were selected as the targets for height estimation. Those locations are shown in Figure 2(a).

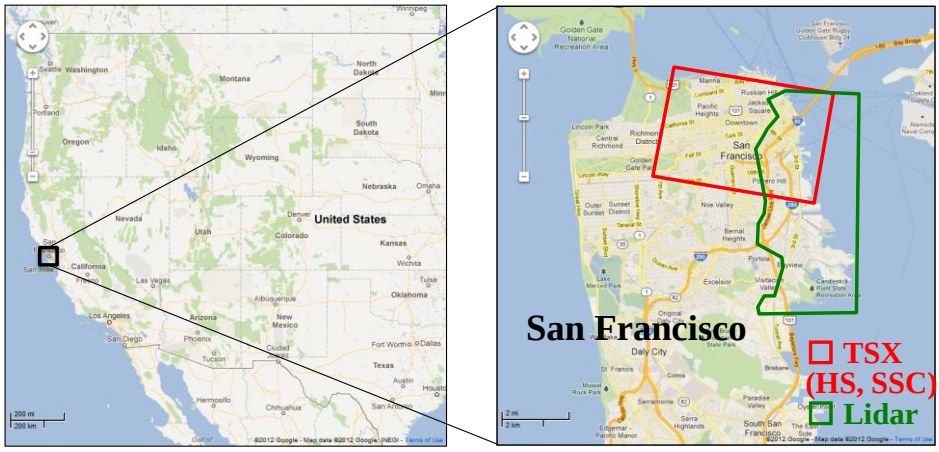

(a) (b)

Figure 1 The study area in San Francisco, CA, U.S.A. (a); shooting areas of TerraSAR-X (TSX) and Lidar (b).

3. METHOD OF DETECTION BUILDING HEIGHT

First, the InSAR analysis was carried out for the two TSX complex data using *SARscape* software. The image taken on December 5, 2007 was set as the master whereas the one on December 27, 2007 as the slave. The Lidar DEM data were introduced to remove topographic fringes. A flattened phase image was obtained by removing orbital fringes and noises using the Goldstein filter. The residual phases were considered as the fringe caused by building heights. A close-up of the residual phase image overlapping on the intensity image is shown in Figure 3(a). It was confirmed that interference fringes were generated within the building layover areas. The theoretical period T [pixel] for one cycle in the interference fringe is expressed by Eq. (1).

$$T = \frac{\lambda H \sin\theta}{2aB_{\perp}} \tag{1}$$

where λ [m] is the radar wavelength and H [m] is the satellite elevation; θ [rad] is the incident angle, a [m/pixel] is the slant range resolution, and $B_{\perp}$ [m] is the vertical distance between the satellite orbits.

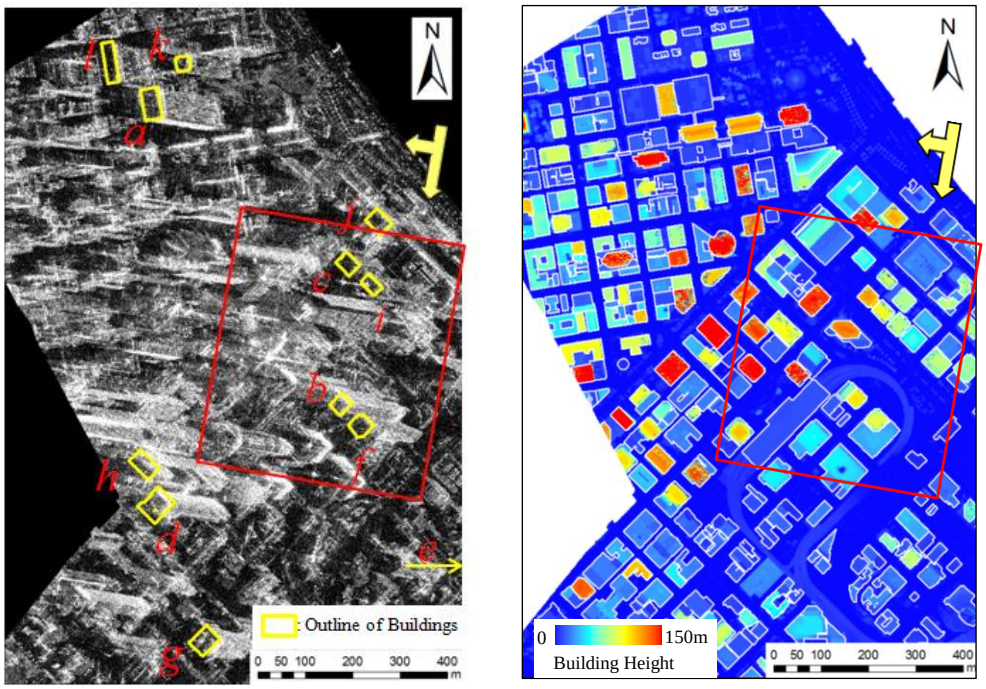

(a) (b)

Figure 2 Geo-coded TSX intensity images in the target area (a) and the reference height obtained by Lidar (b).

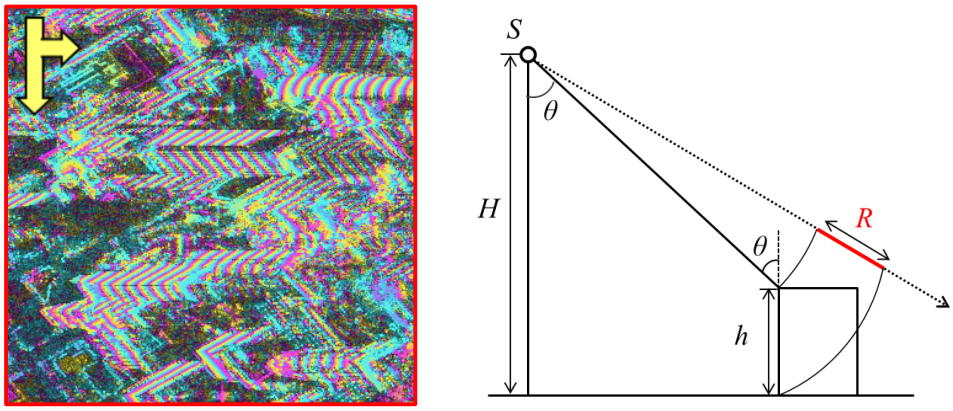

(a) (b)

Figure 3 Phases caused by the building height overlapping on the intensity image (a); a schematic image for geometrical characteristics of a building in SAR images (b).

The incident angle for the master image was 39.9° and the satellite elevation was 501.1 km. The baseline distance between two images is 561.6 m. Thus, T is approximately 10 pixels in the slant-range phase image in theory. Furthermore, the phase gradient ϕ' [rad/pixel] in the range direction for a continuous phase is expressed by Eq. (2).

$$\phi' = \frac{4\pi a B_{\perp}}{\lambda H \sin\theta} \tag{2}$$

According to the acquisition condition, ϕ' equals 0.65 in the obtained phase image. The period T and the phase gradient ϕ' were used as parameters to detect layover areas in this study. After a layover area is determined, a building height can be estimated according to the geometric characteristics. The relationship between the building height and its layover length is shown in Figure 3(b), and can be expressed by Eq. (3).

$$h = \frac{\alpha}{\cos\theta} R \tag{3}$$

In this study, one cycle fringe represents 11.6 m in height.

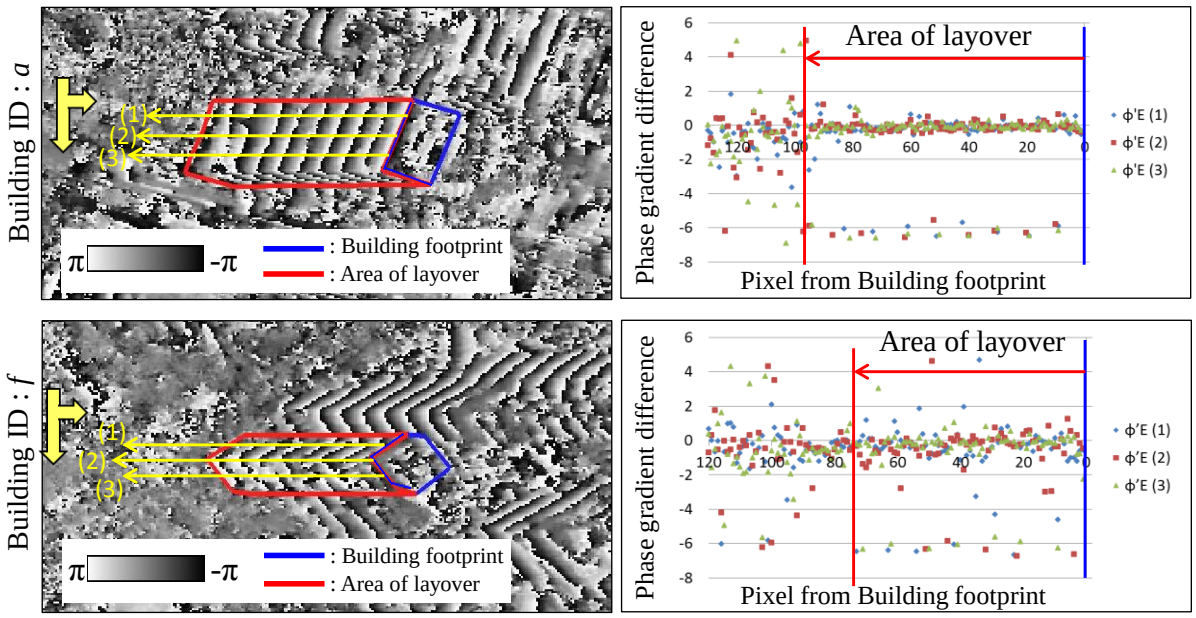

(a) : Interference phase image (b) Change of phase gradient

Figure 4 (a) Footprints of two smaple buildings ***a*** and ***f*** , and their layover areas estimated accoding to the reference height of the Lidar data overlapping on the phase image; (b) the differences (ϕ'_E) between the theoritcial phase gradiant and the acutal values obtained by the InSAR analysis, in three parallar sections shown in (a) for each building.

Two buildings with ID ***a*** and ***f*** were selected to investigate the characteristics of T and ϕ' inside and outside of the layover area. Building ***a*** is the sample for a stable interferogram whereas Building ***f*** is the sample for an unstable one. According to the building height obtained from the Lidar data, the layover area (red frame) was created from the GIS footprint (blue frame) to the range direction, as shown in Figure 4(a). Three sections were selected for each building, which began from the footprint to the sensor direction passing through the layover area. The ϕ' values in these sections were calculated. Then the error ϕ'_E [rad] between the theoretical value and the actual phase gradient was obtained by Eq. (4) and shown in Figure 4(b).

$$\phi'_E = \phi' - 0.65 \tag{4}$$

The ϕ'_E values for Building ***a*** were almost 0 within the layover area except for the gaps of cycles, and varied greatly after passing throug the layover area. Thus, it is easy to identify the boundary of layover from the graph. On the contrary, the ϕ'_E values for Building ***f*** were not stable even in the layover area. It is difficult to determine the boundary of layover only from the phase gradients. Then the period T was taken into account. Since the ϕ'_E for the gap between two cycles is -2π in theory, the pixels with the ϕ'_E less than -4 were regarded as the end of the cycle. In a continuous phase, the distance (T) between two gaps should be 10 pixels according to Eq. (1). Within the layover area of Building ***a***, the gaps repeated regularly in the three sections, and the T values between two gaps were approximately 10 pixels. The gaps became unregularly in the outside of layover. For Building ***f***, the gaps were not regular in some parts of the sections (1) and (2). However, the T values in the section (3) were stable within the layover area. The stable repetition disappeared after passing though the layover area.

From the above observation, the phase gradient is considered to be effective to detect the boundary of layover under the condition with few noises. In contrast, the period of repeat phase cycles could detect the layover area even in the case of noisy phase gradient. However, it is difficult to identify the boundary if the layover area was overlapped by other buildings' layover regions.

A method of detecting layover areas using the phase gradient and the period of phase cycles was proposed in this study. Figure 5 shows the flowchart to estimate the boundary of layover. The detail procedure is explained as follows.

Pre-processing

1) Extract phases within a potential layover area and represent them as $\phi_{i,j}$; where i [pixel] is the line number to the azimuth direction and j [pixel] is the range distance from the footprint.
2) Calculate the phase gradient ϕ'_j in the range direction for each line i.
3) Calculate the phase gradient error $\phi'_{Ei,j}$ between the theoretical value and the obtained phase gradient.

Phase gradient analysis

4) Unwrap the ϕ'_{Ej} to $\phi'_{UE\,j}$ by releasing 2π ambiguity after the gap point where ϕ'_{Ej-1} is less than -4 rad for each line *i*.
5) Calculate the medium value of ϕ'_{UEi} ($Med.|\phi'_{UEi}|$) for the same distance column *j*.
6) When $Med.|\phi'_{UEi}|$ is larger than 0.65, the column value *j* is the length of the layover (*Lp*).

Wrapping point analysis

7) Extract all the wrapping points in the line *i* as $W_{i,\,n}$ (n = 1,2,3…) from the footprint to the sensor direction.
8) If the distance between two wrapping points ($W_{i,\,n} - W_{i,\,n-1}$) is within 3 pixels error from the theoretical value (10 pixels in this study), the phase between these two points was counted as a normal cycle. Parameter *T* in a normal cycle is set as 1, otherwise *T* equals 0.
9) Calculate the average value of *T* (*Ave.T*) for the same distance column j.
10) When *Ave.T* is lower than 0.1, the column value *j* is the length of the layover (*Lw*).

Final decision

11) The smaller value between L_p and L_w is considered as the final length of the layover area and used to estimate the building height.

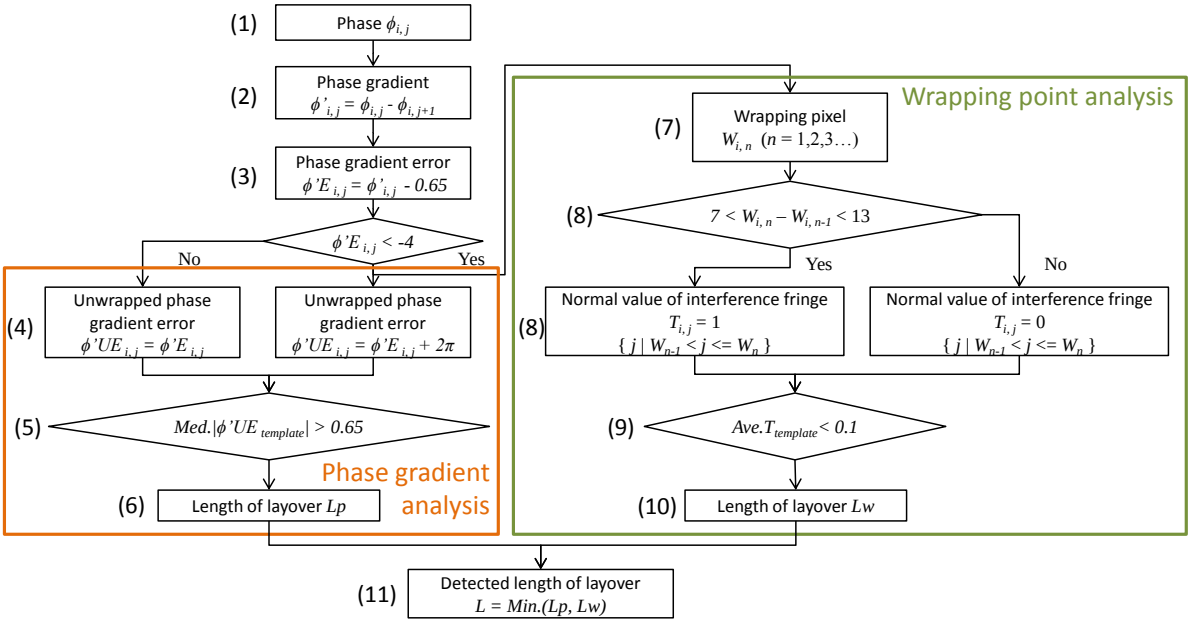

Figure 5 Flow of the proposed method to detect layover areas.

4. RESULT OF DETECTING HEIGHT AND COMPARATIVE REVIEW

The heights of 12 target buildings were detected by the proposed method and the result was listed in Table 1. To verify the accuracy of the obtained values, reference building heights were obtained from the Lidar data. A reference height was calculated as the average difference between the DSM and the DEM data within a building footprint. The highest target building is about 125 m regarded as 42-stories (the height of one story is counted 3 m), whereas the lowest one is 55 m as 18-stories. The comparison of the obtained results and the reference is shown in Table 1 and Figure 6. The minimum error of our result is -1.5m for Building ***i***, and the maximum error is -18.2 m for Building ***g***. The coefficient of determination is 0.87. The average difference is 6.94 m and the root mean square (RMS) error is 8.36 m, respectively.

The error of the proposed method is less than the height of one phase cycle, which is 11.6 m. 75% of the building heights could be detected within 10 m accuracy. The detected result is considered as high accuracy, compared with the original heights. However, 75% of the buildings were estimated lower than their reference heights. It is considered that the phases at the end of the layover area were affected by noises from machineries and equipment on the roof, and were difficult to be extracted as a part of the layover area. Actually, it is confirmed from the aerial photograph that most of the high-rise buildings have outdoor units of air-conditioning machines on the roofs. On the contrary, the heights of Buildings ***c*** and ***d*** were detected as 10 m higher than their references. These error occurred when the target layover area was overlapped with other layovers of the surrounding buildings

Table 1 Comparison of the detected results and the reference heights from the Lidar data (unit: m).

Building ID	*a*	*b*	*c*	*d*	*d*	*e*	*f*	*g*	*h*	*i*	*j*	*k*
Detected height	110.0	95.7	64.6	110.0	62.2	87.3	65.8	128.0	88.5	108.8	75.4	58.6
Reference height	116.0	106.0	55.0	99.0	67.0	90.0	84.0	125.0	90.0	115.0	77.0	67.0
Error	-6.0	-10.3	9.6	11.0	-4.8	-2.7	-18.2	3.0	-1.5	-6.2	-1.6	-8.4

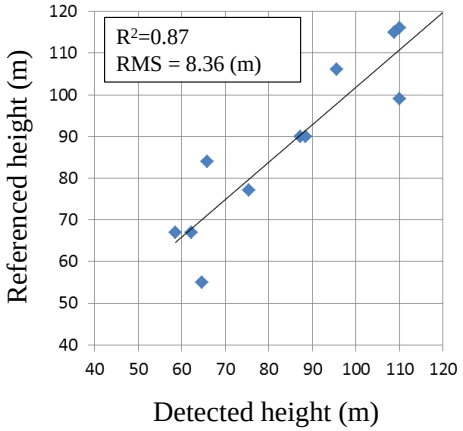

Figure 6 Comparison of the heights obtained by the proposed method and the reference heights data.

5. CONCLUSION

In this study, a method for detecting heights of high-rise buildings was proposed on the basis of an InSAR analysis and geometrical characteristics. The method was conducted using two-temporal TerraSAR-X images and a GIS building footprint data in the Skyscrapers zone of San Francisco. Interference phases caused by building heights were calculated using the InSAR analysis, and their characteristics inside and outside of the layover area were investigated for several sample buildings. Then the heights of 12 buildings over 50 m were detected by the obtained parameters. Comparing with the reference heights obtained from Lidar data, the average difference was 6.94 m and the RMS error 8.36 m, which is less than one cycle height (11.6 m). 75% of building heights were detected as lower than the reference due to machineries and equipment on the roof. Some overestimation occurred since layover areas were overlapped by other buildings. The accuracy of the proposed method will be improved by applying it to more examples in the future.

ACKNOWLEDGMENT

The TerraSAR-X images and Lidar data used in this study were provided by the 2012 IEEE Geoscience and Remote Sensing Society (GRSS) Data Fusion Contest.

REFERENCES

Bolter, R., and Leberl, F., 2000. Detection and reconstruction of human scale features from high resolution interferometric SAR data. In: Pro. 15th Int. Conf. Pattern Recog., 4, pp. 91–294.

Brunner, D., and Lemoine, G., 2010. Building height retrieval from VHR SAR imagery based on an iterative simulation and matching technique. IEEE Trans. Geosci. Remote Sens., 48 (3), pp. 1487–1504.

Building footprints for the City and County of San Francisco as of June 2011, Retrieved August 18, 2014 from https://data.sfgov.org/Facilities-and-Structures/Building-Footprints-Zipped-Shapefile-Format-/jezr-5bxm

Franceschetti, G., Guida, R., Iodice, A., Riccio, D., and Ruello, G., 2007. Building feature extraction via a deterministic approach: Application to real high resolution SAR images. In: Proc. IEEE IGARSS, pp. 2681–2684.

Franceschetti, G., Iodice, A., and Riccio, D., 2002, A canonical problem in electromagnetic backscattering from buildings. IEEE Trans. Geosci. Remote Sens., 40 (8), pp. 1787 Sens.

Liu, K., Balz, T., and Liao, M., 2009. Building height determination by TerraSAR-X backscatter analysis in dense urban areas. In: Proc. 2009 ACRS.

Liu, W., Yamazaki, F., 2013. Building height detection from high-resolution TerraSAR-X imagery and GIS data. Proceedings of 2013 Joint Urban Remote Sensing Event, IEEE, CD-ROM, pp. 33-36.

Thiele, A., Cadario, E., Schulz, K., Thoennessen, U., and Soergel, U., 2007. Building recognition from multi-aspect high-resolution InSAR data in urban areas. IEEE Trans. Geosci. Remote Sensing, 45 (11), pp. 495–505.

Yamazaki, F., Liu, W., Mas, E., Koshimura, S., 2013. Development of building height data from high-resolution SAR imagery and building footprint. Proceedings of the 10th International Conference on Structural Safety and Reliability, CD-ROM, 7p.